Decadal Changes in the 50-Year GECCO Ocean Synthesis

Armin Köhl and Detlef Stammer
Institution of Oceanography, Hamburg, Germany, armin.koehl@zmaw.de

The German partner of the "Estimating the Circulation and Climate of the Ocean" (GECCO) consortium provided a dynamically consistent estimate of the time-varying ocean circulation over the 50-year period 1952-2001. The estimate results from a synthesis of most of the ocean data sets available during this 50-year period with the ECCO/MIT ocean circulation model. This GECCO estimate is analysed here with respect to decadal and longer term changes in in sea level and meridional overturning circulation (MOC). A special focus is on the maximum MOC values at 25°N. Over this period the syntheses stays within the error bars of Bryden et al., but reveals a general increase of the MOC strength. The variability of the meridional overturning is decomposed into contributions from different processes. Regional changes in sea level are predominantly associated with an intensification of the subtropical gyre circulation and a corresponding redistribution of heat. The horizontal advection of heat due to an increase in wind stress curl is found to explain a major fraction of the estimated regional sea level trends over the last 40 years.

1 Optimization

The approach is identical to the 11 year ECCO estimation (Köhl et al., 2007b) in which initial temperature and salinity conditions as well as the time-dependent surface fluxes of momentum, heat and freshwater are adjusted by the adjoint method in order to bring a global 1 degree model into agreement with observations.

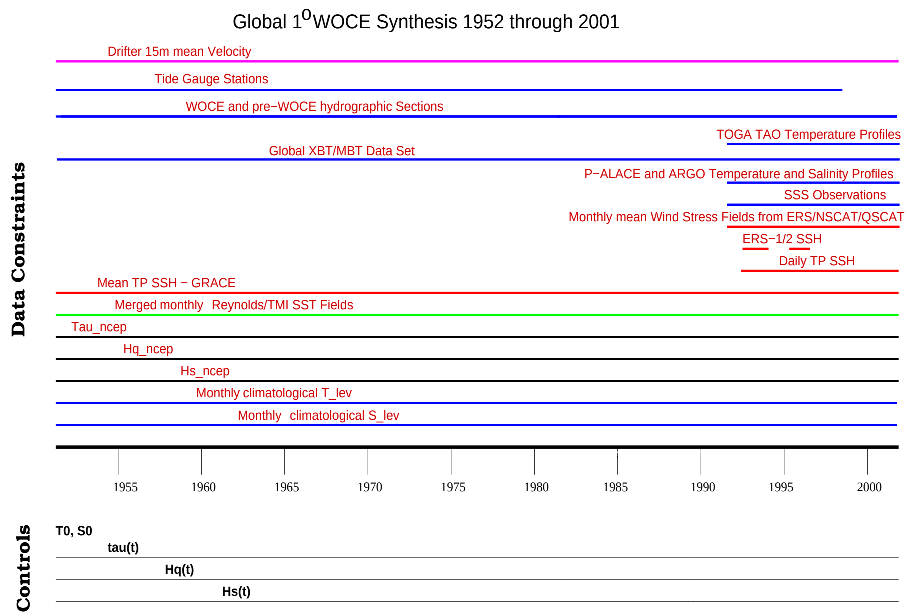

Figure 1: Schematic of the optimization. The upper part shows the data constraints imposed on the model. The lines indicate times when data is available, mean or climatological data is shown as being available throughout the whole period. The lower part summarizes the control parameters that were changed during the optimization.

Before 1992 the state is mainly constrained by an extensive data base of subsurface XBT and MBT measurements whereas only after 1992 the same data rich data base is available as for the 11 year estimation. We show results of iteration 23.

2 Sea level Changes

During the past 20 years, substantial progress has been made in analyzing and understanding decadal variability and multi-decadal trends in global ocean heat content and thermosteric sea level. Church et al. (2001) documented the widespread results of early thermal expansion estimates of the order of 1 mm/yr. For the last decade a clear contribution of freshwater input could be shown (Willis et al., 2004). Church et al. (2004) attempted to provide an improved estimate of sea level change over the last 50 years. To overcome the inadequate data distribution, a promising approach is to synthesize all available data into one dynamically consistent estimate of the evolving ocean by merging them with a circulation model through dynamically consistent data assimilation. We will thus focus on regional and global sea level changes on decadal and longer time scales as they result from the GECCO estimate (see also, Köhl and Stammer, 2006)

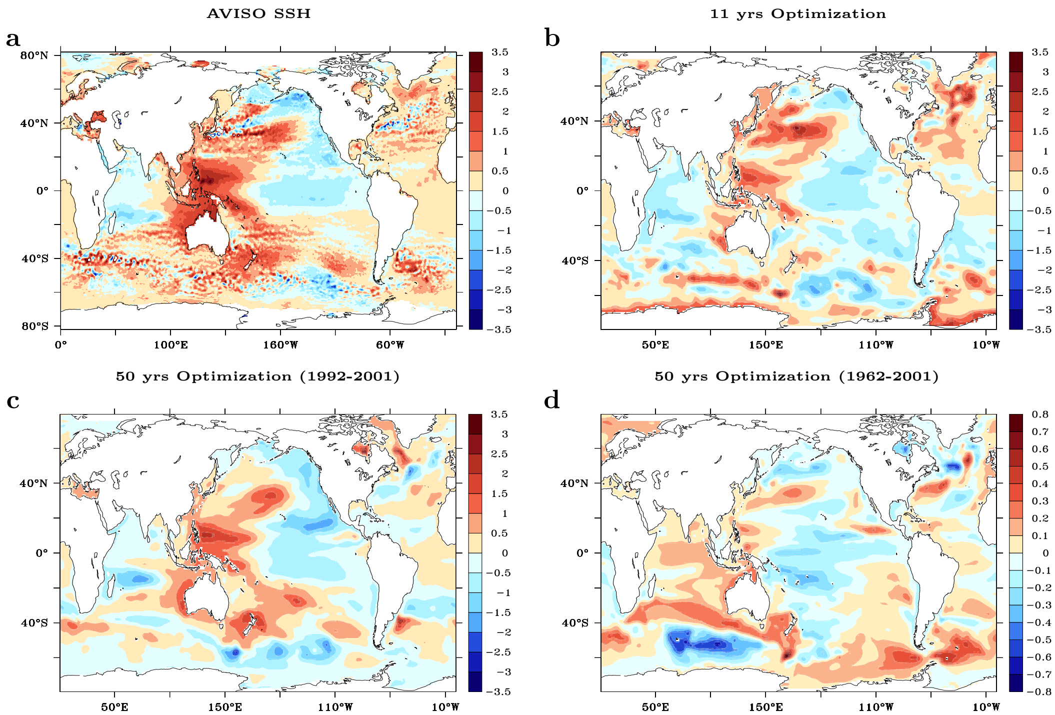

Figure 2: SSH trends in cm/year from altimeter data and ocean state estimations. Top row: mapped AVISO SSH (left) and SSH form the 11 years optimization (right). Bottom row: SSH trend from the 50 years optmization for the period 1962-2001 (left) and the last decade (1992-2001) (right).

The pattern of trends calculated over the period 1962 - 2001 is shown in Fig. 2d. They were calculated here and subsequently by fitting a least-squares line into the time series of monthly mean values, including the seasonal cycle. In contrast to the period after 1992, where altimeter data provide an excellent constraint, the estimation of the trends before 1992 relies mainly on SST and upper ocean thermal data (XBTs and MBTs). It is therefore reassuring that the spatial patterns nevertheless are similar to those estimated by Church et al. (2004) from tide gauge data over the period 1950-2000.

The period after 1990 is marked by an unprecedented sampling of ocean sea surface and hydrography, especially through Repeat Hydrography and the ARGO network and through the advent of high-precision satellite altimetry. The impact of altimetry is especially large because of its ability to provide accurate observations of global sea level patterns and trends. An example is provided in the top panel of Fig. 2a showing an estimate of the trend in SSH based on altimeter data estimated for the period 1992 through 2001.

Fig. 2c shows the model adjustment in sea surface height as it results from the 50-year run, but estimated now only over the last 10 years, 1992 - 2001. Amplitude and pattern of the estimated trend closely match the changes observed by TOPEX/Poseidon data during the same period (top panel). The largest changes are of the order of more than $\pm$ 2 cm per year which can be found in the Pacific, the Labrador Sea, the Malvinas, and over the Pacific sector of the ACC. Positive SSH changes are in the western and negative changes in the eastern Pacific. For the Indian Ocean, the opposite can be seen. In comparison to the previous 11-year ECCO optimization (Fig. 2b) described by Köhl et al. (2007b), the estimate resulting from the 50-year run clearly is superior in simulating the observed SSH trend during the last decade. As an example, the southern Pacific in the GECCO run shows roughly the observed increase that is mostly absent from the shorter run. Likewise the Southern Ocean and the subpolar North Atlantic show more realism in the SSH trend in the GECCO run, which is less obvious from the shorter ECCO run. Both examples demonstrate the impact of the model initial adjustments on estimates of decadal changes that negatively impact the shorter ECCO runs, underpinning the advantage of long estimation runs.

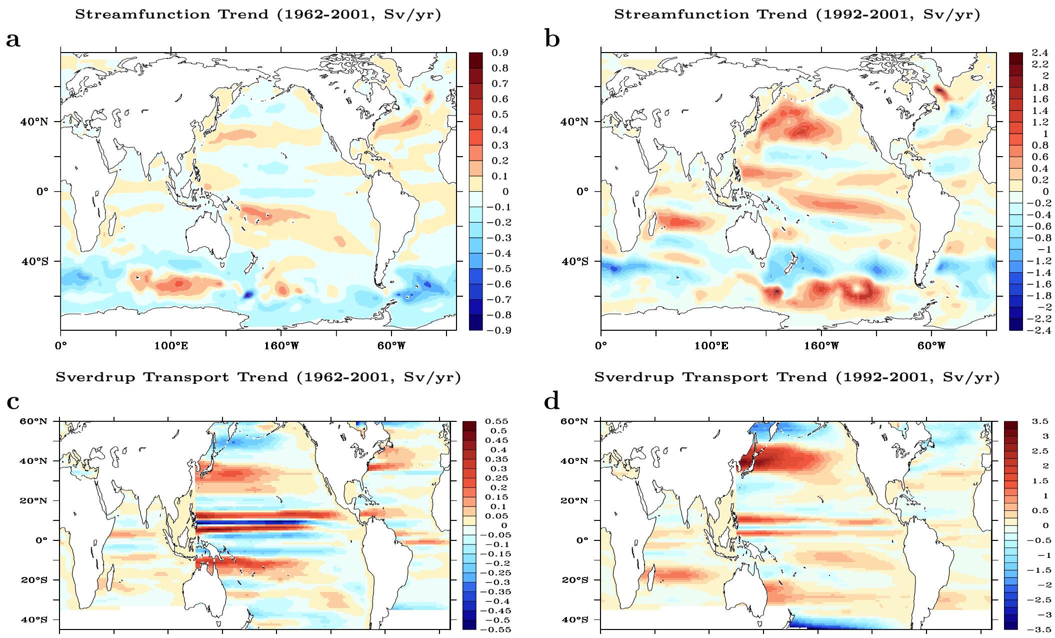

Figure 3: Trends of the barotropic streamfunction for a) the period 1962-2001 and for b) the period 1992-2001. Bottom row: Trends of the Sverdrup transports calculated from the corresponding wind stress curl estimation for c) the period 1962-2001 and for d) the period 1992-2001. The Estimates from 50-year optimization are in Sv/yr.

Focusing on the South Pacific, Roemmich et al. (2007) suggested that an increase in the circulation of the South Pacific subtropical gyre led to a sea surface height increase of up to 12 cm between 1993 and 2004 due to increased wind stress curl associated with an increase in the atmosphere's Southern Hemisphere annular mode (SAM).

To confirm that the changes in the barotropic streamfunction are driven by changes in the wind field according to the barotropic vorticity equation, we show in the lower part of Fig. 3 the trend in the pure Sverdrup circulation as it results from the GECCO wind stress fields over the same periods. For that purpose the Sverdrup transport streamfunction was evaluated from monthly mean GECCO wind stress fields according to

$$\Psi_{Sv}(x,y,t) = \frac{1}{\beta\rho_0}\int_x^{x_{east}} \nabla\times\tau(x,y,t) \quad (1)$$

with $\beta = \partial f/\partial y$, ρ_0 a reference density, and τ the wind stress. Trends in the Sverdrup transport streamfunction were calculated subsequently from the monthly mean fields. Patterns of the trends of the Sverdrup transports correspond reasonably well with the trend of the streamfunction, especially in the eastern parts of mid-latitudes gyres. In general the trends of the Sverdrup transports overestimate the streamfunction trend since bottom topography and stratification is not considered.

3 MOC changes

The fundamental importance of MOC variations to northern hemisphere climate changes and possible impact on society are of paramount interest especially since recent model studies from (e.g.) Manabe and Stouffer (1993) hypothesized that the anthropogenic increase in the atmospheric concentration of CO_2 and other greenhouse gases could lead to a measurable reduction in MOC strength in the Atlantic over the next century. Estimates of MOC changes at 25°N in the North Atlantic were investigated recently by Bryden et al. (2005) who extended the previous time series through 2004. The authors report a significant reduction in MOC strengths of about 30% in subsequent years.

In order to facilitate a direct comparison with recent results provided by Bryden et al. (2005) for 25°N, we show in Fig. 4 a time series of the maximum MOC at 25°N (here and in all subsequent figures, the curves were smoothed with a one year running mean filter). The figure suggests that since around 1960 the MOC slightly increased in strength throughout most of the remaining GECCO integration period. At the end of 2002 an overall increase of about 2 Sv is reached which takes mainly place during the late 1970s. The overall variability pattern on shorter timescales, including the initial drop in the MOC strength, is quite similar in both runs. Apart from the additional increase after the 1980s in the reference run, we note an oscillation on a decadal time scale in the transport differences imposed through the ocean data. As already discussed by Köhl et al. (2007b),

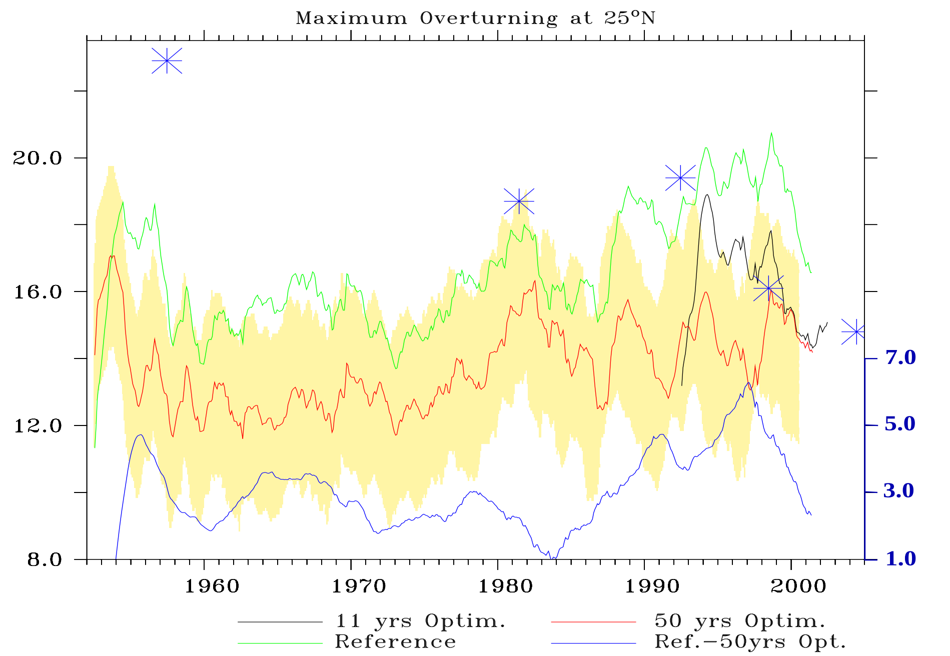

Figure 4: Maximum MOC at 25°N for the reference (green), the 50 yrs optimization (red) and the earlier 11year optimization (black). The yellow shading indicates one standard deviation of the subannual variability of the optimization which amounts to 2.4 Sv and the difference between the reference and the 50 yrs optimization is shown in blue with an offset for clarity of the plot. Values of the estimation of the MOC in 1000 m depth by Bryden et al. (2005) are indicated by asterisks.

the slow adjustment part of the MOC variability is related to a transition to a state that the model is able to maintain wherefore a large fraction of the variability during the first decade has to be considered as unrealistic. During the later 4 decades our analysis remains within the 6 Sv error bar of the measurements of Bryden et al. (2005). Only their 1957 estimate is an exception but falls within the disregarded first decade. This estimate is also crucial for their conclusion that the MOC is decreasing. Both estimates remain therefore consistent, although our simulated variability and positive trend does not particularly agree with their measurements. A lagged-correlation analysis provides a statistical tool to identify mechanisms leading to actually simulated MOC variability. In order to explore the sources of variability for the MOC, we show in Fig. 5 the time series of the maximum MOC at 48°N together with a regression of the density from a region south of the Denmark Strait and of the Denmark Strait overflow with the MOC curve from 48°N, respectively. Also shown is the regression of the NAO index on the 48°N MOC changes. The MOC at 48°N shows after the initial decline an increase after 1960 with a second major increase in the mid 1970s. Superimposed on this long term trend is interdecadal variability. For the last decade we added results from Lumpkin et al. (2007) wich describe in agreement with the present estimate a maximum MOC around 1996/1997 and a decline thereafter. Lumpkin et al. (2007) also provide an error bar for their estimations (about 1-2 Sv) and explore the sensitivity to different assumptions (about 1-2 Sv). Apart from the long term trends, a fraction of this interdecadal variability is represented by the 3 regressions. Regression coefficients between the 48°N MOC timeseries and the above regressions are summarized in Table 1. In addition, similar parameters are shown for the mixed layer depth and density in the

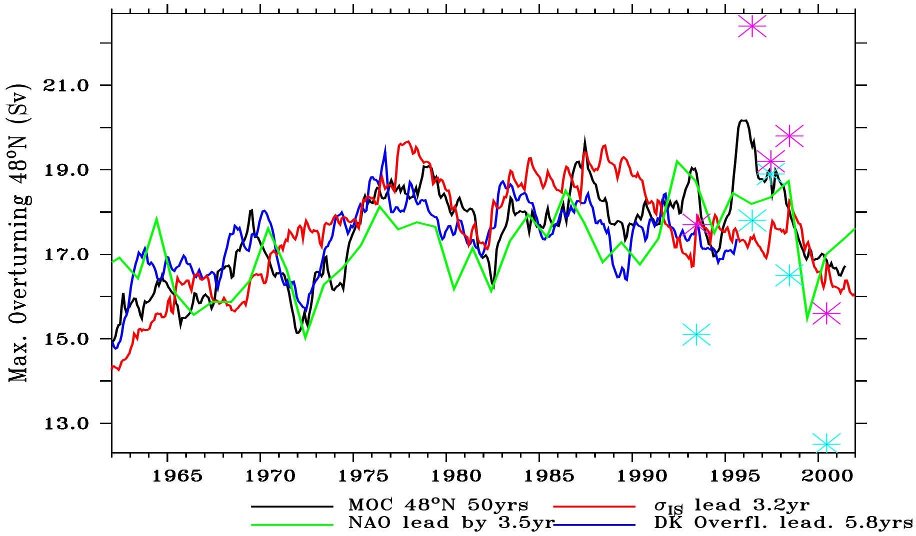

Figure 5: Time series of the maximum MOC at 48°N (black) plotted together with a regression of the density in the Irminger Sea (σ_{IR}, red) and the Denmark Strait overflow on the MOC at 48°N (blue). Overlayed as purple and blue stars are the MOC estimates based on WOCE repeat hydrographic lines by Lumpkin et al. (2007) from a thermal wind and a box inverse model, respectively. The NAO time series shifted by 3.5yr is shown in green.

LS, the density of the Irminger Sea and the local Ekman transport at that latitude.

Table 1: Correlation coefficients and lags in years between the MOC at 48°N and components of the flow field. The density in the Labrador and in the Irminger Sea are averages at 900m over the region 65°W-45°W/52°N-66°N and 45°W-10°W/52°N-66°N, respectively. MLD_{LS} is the maximum mixed layer depth in the LS.

Corr. C. / Lead./yrs	NAO	MLD_{LS}	Ekman	σ_{LS}	σ_{IR}	DK Overfl.
MOC 48°N	0.58 3.5	0.3 0.25	0.08 0	0.89 2.2	0.91 3.2	0.83 4.8

In contrast to Böning et al. (2006), we find a low correlation between the 48°N MOC strength and the maximum mixed layer depth in the Labrador Sea (LS) (r=0.3). Instead an enhanced correlation to the density at 900 m in the LS (r=0.89) and an even higher correlation to the density in 900 m depth from south of the overflows (r=0.91) is found. The latter is supported by the high correlation between the MOC at 48°N and the Denmark Strait overflow variability (r=0.83, with lead 4.8 yr). Together with the lower correlation to the mixed layer depth variability in the LS, this indicates that the correlation to the density variability in the LS is actually substantially caused by density variations that are created by the overflows and advected into the LS rather than created locally. Both mechanisms are consistent with a correlation of the NAO index on the MOC changes at 48° N. Previously, Eden and Willebrand (2001) also investigated the response of MOC changes at 48° N to atmospheric forcing anomalies over the LS and reported an increase in MOC strength after a lag of 2-3 years relative to enhanced convection activity during high NAO states. In the absence of overflow measurements, the NAO index appears to be a good proxy for changes of the MOC at 48°N and 3 years years later also at 25°N.

4 Conclusion

The global estimate of the ocean state over the period 1992-2002 by Köhl et al. (2007b) was extended into the past to cover the 50-years period 1952-2001. Longterm state estimation efforts are necessary to investigate changes in the circulation especially the MOC, since the adjustment to the overflows dominate processes during the first decade of the simulation. Regional changes in sea level are predominantly associated with an intensification of the subtropical gyre circulation and a corresponding redistribution of heat. The horizontal advection of heat due to an increase in wind stress curl is found to explain a major fraction of the estimated regional sea level trends over the last 40 years. However, the mechanisms appear different during the last decade when in some regions changes in surface heat flux may explain as much as 50% of the sea level changes. Over the last four decades we find a general increase of the MOC at 25°N by about 2 Sv. Although it disagrees with Bryden et al. (2005) who reported a reduction by 30% over the last 50 years, our estimate remains within error bars and thus consistent with their estimates. The reason for this seeming paradox is that the 1957 estimate is necessary for the significance of their reduction but is excluded from the comparison over the shorter period. Other model results also support a MOC increase, which can be understood since a large fraction of the MOC variations can be described as lagged response to NAO variability (Eden and Willebrand, 2001).

References

Böning, C. W., M. Scheinert, J. Dengg, A. Biastoch, and A. Funk, 2006: Decadal variability of the subpolar gyre transport and its reverberation in the North Atlantic overturning, *Geophys. Res. Lett.*, **33**, L21S01.

Bryden, H. L., H. R. Longworth, and S. A. Cunningham, 2005: Slowing of the Atlantic meridional overturning circulation at 25^o N, *Nature*, **436**, 655–657.

Church, J. A., J. M. Gregory, P. Huybrechts, M. Kuhn, K. Lambeck, M. T. Nhuan, D. Qin, and P. L. Woodworth, 2001: *The Scientific basis. Contribution of working group 1 to the third assesment report of the Intergovernmental panel on clate change*, Climate Change 2001: J. T. Houghton et al. Eds., Cambridge University Press, Cambridge, 639–694.

Church, J. A., N. J. White, R. Coleman, K. Lambeck, and J. X. Mitrovica, 2004: Estimates of the regional distribution of sea level rise over the 1950-2000 period, *J. Climate*, **17**, 2609–2625.

Dickson, R. R., and J. Brown, 1994: The production of North Atlantic deep water: Sources, rates and pathways, *J. Geophys. Res.*, **99**, 12319–12341.

Eden, C., and J. Willebrand, 2001: Mechanism of interannual to decadal variability of the north atlantic circulation, *J. Climate*, **14**, 2266–2280.

Köhl, A., R. Käse, D. Stammer, and N. Serra, 2007a: Causes of changes in the Denmark Strait Overflow, *J. Phys. Oceanogr.*, **37**, 1678–1696.

Köhl, A., and D. Stammer, 2004: Optimal observations for variational data assimilation, *J. Phys. Oceanogr.*, **34**, 529–542.

Köhl, A., and D. Stammer, 2006: Decadal sea level changes in the 50-year GECCO ocean synthesis, *J. Climate*, in press.

Köhl, A., D. Stammer, and B. Cornuelle, 2007b: Interannual to decadal changes in the ECCO global WOCE synthesis, *J. Phys. Oceanogr.*, **37**, 313–337.

Lumpkin, R., K. G. Speer, and K. P. Koltermann, 2007: Transport across 48^{o}n in the Atlantic Ocean, *J. Phys. Oceanogr.*, **37**, in press.

Manabe, S., and R. J. Stouffer, 1993: Century-scale effects of increased atmospheric CO2 on the ocean-atmosphere system, *Nature*, **364**, 215–218.

Roemmich, D., J. Gilson, R. Davis, P. Sutton, S. Wijffes, and S. Riser, 2007: Decadal spin-up of the South Pacific subtropical gyre, *J. Phys. Oceanogr*, **37**.

Willis, J. K., D. Roemmich, and B. Cornuelle, 2004: Interannual variability in upper ocean heat content, temperature, and thermosteric expansion on global scales, *J. Geophys. Res.*, **109**, C12036.